Assessment and Prediction of Vestibular Schwannoma Response to Anti-angiogenic Therapy in Neurofibromatosis Type 2 Patient Using Low Dose High Temporal Resolution DCE-MRI

Ka-Loh Li[1], Alan Jackson[1], and Xiaoping Zhu[1]

[1]*WMIC, University of Manchester, Manchester, Great Manchester, United Kingdom*

Target Audience DEC-MRI experts, oncologists and radiologists

Purpose The dual temporal resolution dynamic contrast imaging (DTR), consists of two series, the 'prebolus' - low dose high temporal (LDHT), and the 'main' - full dose high spatial (FDHS) resolution. The LDHT of DTR is initially designed for extraction of the arterial input function (AIF) for the calculation of pharmacokinetic parametric maps from the FDHS, including transfer constant (K^{trans}), fractional plasma volume (v_p) and fractional volume of extra-vascular extra-cellular space (v_e). Much lower dose, e.g. 1/5 of standard dose, was used for LDHT, avoiding MR signal saturation in large vessels, where AIF was extracted[1]. However, solely use of LDHT for cancer diagnosis was overlooked until quite recently[2-5]. The aim of this study is to exploit the use of the LDHT for clinical management of patients with tumors, e.g. assessment and prediction of treatment efficacy in vestibular schwannomas (VS) and meningiomas in patients with type II neurofibromatosis (NF2).

Methods DTR were collected in twelve consecutive NF2 patients with a total of 20 VS, who underwent an anti-vascular endothelial growth factor antibody bevacizumab treatment. Patients were imaged pre-treatment (day 0) and 3 months (day 90) following treatment. A low dose of dotarem (0.02 mmol/kg) was used as prebolus for the LDHT. A standard dose (0.1 mmol/kg) was then administered for the FDHS. Varying flip angle acquisitions were performed prior to the LDHT for the native longitudinal relaxation rate ($R1_N$) mapping, and again prior to the FDHS. 4D tissue CA concentration images, $C(t)$, from the LDHT and FDHS were then calculated and fitted to a two-compartment kinetic model. 3D maps of K^{trans}, v_p and v_e were calculated. 3D eigen images were also calculated from the 4D LDHT and FDHS using the principal components analysis featuring the maximum contrast enhancement of tumors. VS were segmented from the FDHS using a supervised automatic edge detection program. The differences of K^{trans}, v_p, v_e and $R1_N$ of VS before and after treatment were evaluated using Wilcoxon signed rank tests for the subgroups of responders and non-responders. Pre-treatment values of tumor volume, $R1_N$, and the pharmacokinetic matrices (K^{trans}, v_p and v_e) calculated from LDHT and FDHS were used as the predictors in a logistic regression and cross validation analysis.

Results FDHS portrayed VS and meningioma distinctively (Fig. 1b), but the LDHT did not (Fig. 1a). Poor presentation of tumors is due to low concentration of dotarem in tumors. Eigen images associated large eigen values maximized tissue contrast and highlighted the enhanced tumors from LDHT (Fig. 1c), showing that adequate contrast-to-noise ratio was there but hidden. A small meningioma was not shown on the enhanced image or the 4th eigen image with the LDHT. K^{trans} image derived from the LDHT has detected the small meningioma (arrow), which is highly permeable (Fig, 1e). There is no contamination from the arteries on K^{trans} map of LDHT, but severe on FDHS (Fig. 1f). LDHT separated extra- from intra-vascular space, and FDHS could not. Figure 2 compares pharmacokinetic parameters and $R1_N$ of the VS measured on day 0 and day 90 from the groups of responders (left 2 boxes of each panel) and non-responders (right 2 boxes of each panel) to assess the treatment effects. Amid pharmacokinetic parameters calculated from LDHT, only K^{trans} were significantly reduced 90 days after treatment (p = 0.003). Conversely, FDHS showed reduction of both K^{trans} (p = 0.034) and v_p (p = 0.001). The panel at the right upper corner of Fig. 2 shows significant increase of $R1_N$ of the responder group after treatment (p = 0.027). None of those variables from the 'non-responder' group showed difference between day 0 and 90 days after treatment The pre-treatment volumes of the VS responders were significantly larger than VS non-responders (p = 0.0003). Pre-treatment K^{trans} from LDHT of VS responders was significantly higher than VS non-responders (p = 0.012). Pre-treatment v_p from FDHS of VS responders was significantly higher than VS non-responders (P = 0.002). The VS responders had significantly longer T1 relaxation time (p < 0.0001) and larger volume (P = 0.0003) than VS non-responders. Finally, we tested the extent to which LDHT measures improved classification of responders and non-responders as compared with that based on using FDHS alone. Table 1 lists the sensitivity, specificity, and overall classification of responders and non-responders for the combinations, whereas the explanatory variables and covariates were estimated together using the general linear regression model. The K^{trans} (LDHT) yielded an overall classification of 76% with a sensitivity of 85% and specificity of 62%. A combination of K^{trans} (LDHT) and v_p (LDHT) achieved a classification of 88% with a sensitivity of 98% and specificity of 74%. For the model with only v_p (FDHS) as an explanatory variable, prediction of group membership was significant, yielding an AUC of 0.90. However, adding K^{trans} as a covariate led to only a slight increase of the AUC to 0.91. The pre-treatment $R1_N$ was revealed the best predictor with overall classification of 90%, sensitivity of 92% and specificity of 88%.

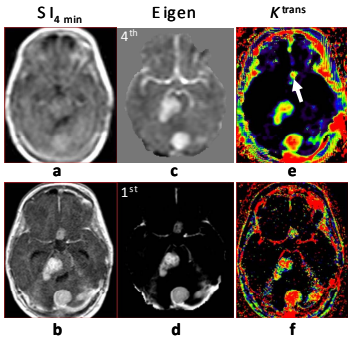

Figure 1. Pre-treatment images and maps of VS and meningioma from a NF2 patient. Left: enhanced frames 4 min post-injection; Middle: eigen images (4th for LDHT; 1st for FDHS), Right: K^{trans} maps from LDHT and FDHS.

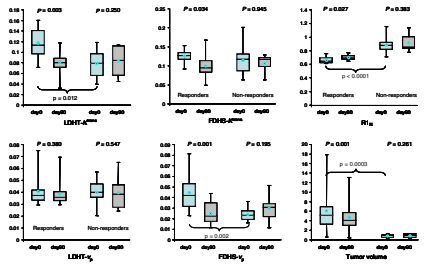

Figure 2. Comparison of treatment-induced changes between 'responders' and 'non-responders', showing median (bar), inter-quartile range (box), extreme (whiskers) and mean (diamond). Brackets noticed levels of differences (p values) between 'responders' (left) or 'non-responders' (right) on day 0.

Table 1. Classification of VS responders and non-responders based on the leave-one-out logistic regression analysis of LDHT and FDHS parameters.

	predictors	Prediction	Sensitivity	Specificity	AUC
LD	K^{trans}	0.76±0.03	0.85±0.05	0.62±0.10	0.83±0.02
	K^{trans} + v_p	0.88±0.03	0.98±0.05	0.74±0.05	0.85±0.03
	$R1_n$	0.91±0.03	0.92±0.03	0.88±0.04	0.99±0.00
FD	v_p	0.78±0.04	0.78±0.05	0.78±0.07	0.90±0.02
	v_p + K^{trans}	0.78±0.05	0.78±0.06	0.78±0.06	0.91±0.01
VS volume		0.95±0.01	0.92± 0.02	1.00±0.00	0.95±0.01

Discussion This study exploits the overlooked prebolus low dose DCE-MRI, and shows how the new approach can improve identification of VS responders, who may benefit from the antiangiogenic treatment. K^{trans} maps from LDHT exhibited supremacy to FDHS in separating the extra- from intra-vascular spaces. Combined use of K^{trans} and v_p has improved identification of the VS responders. Conversely, adding FDHS K^{trans} to v_p has little effect, indicating again the FDHS inferior in separation of K^{trans} from v_p. The $R1_N$ was not initially considered as the top candidate for the prediction, but the new discovery of effectiveness of $R1_N$ in prediction of VS responders was not entirely a surprise. Longer T1 time was observed in progressive VS by previously investigators[6,7], probably due to the wide extra-cellular space in the growing VS. In conclusion, we recommend DTR. The combined LDHT and FDHS can provide new biological insights into the treatment of patients with tumor.

References 1) Canet E, et al, JMRI 1995, 411; 2) Baxter S et al, JMRI 2009,1317; 3) Larsson HB et al, MRM, 2009, 1270; 4) Makkat S, JMRI 2010, 556; 5) Taheri S et al, MRM 2011, 1036; 6) Zhu XP et al, JMRI 2000, 575; 7) Watabe T, AJNR 1989, 463.